Metabolite Profiling Identifies a Key Role for Glycine in Rapid Cancer Cell Proliferation

Mohit Jain *et al.*

Science **336**, 1040 (2012);
DOI: 10.1126/science.1218595

Science (print ISSN 0036-8075; online ISSN 1095-9203) is published weekly, except the last week in December, by the American Association for the Advancement of Science, 1200 New York Avenue NW, Washington, DC 20005.

conformation of guide RNAs in a manner that is not seen for guide DNAs in bacteria. Moreover, the tryptophan-binding sites in the PIWI domain form a likely interaction surface for additional RNA-induced silencing complex components for which no known homologs exist in the prokaryotic kingdom. The structures presented here extend studies of the prokaryotic into understanding Argonaute in humans. Bridging this gap is an essential step toward leveraging structural information for design and delivery strategies for silencing human disease factors using RNAi.

References and Notes

1. J. Liu *et al.*, *Science* **305**, 1437 (2004).
2. G. Meister *et al.*, *Mol. Cell* **15**, 185 (2004).
3. I. Behm-Ansmant *et al.*, *Genes Dev.* **20**, 1885 (2006).
4. J. E. Braun, E. Huntzinger, M. Fauser, E. Izaurralde, *Mol. Cell* **44**, 120 (2011).
5. M. R. Fabian *et al.*, *Nat. Struct. Mol. Biol.* **18**, 1211 (2011).
6. J. J. Song, S. K. Smith, G. J. Hannon, L. Joshua-Tor, *Science* **305**, 1434 (2004).
7. Y. Wang *et al.*, *Nature* **456**, 921 (2008).
8. Y. Wang *et al.*, *Nature* **461**, 754 (2009).
9. Y. Wang, G. Sheng, S. Juranek, T. Tuschl, D. J. Patel, *Nature* **456**, 209 (2008).
10. Y. R. Yuan *et al.*, *Mol. Cell* **19**, 405 (2005).
11. J. B. Ma *et al.*, *Nature* **434**, 666 (2005).
12. J. B. Ma, K. Ye, D. J. Patel, *Nature* **429**, 318 (2004).
13. A. Lingel, B. Simon, E. Izaurralde, M. Sattler, *Nature* **426**, 465 (2003).
14. J. J. Song *et al.*, *Nat. Struct. Biol.* **10**, 1026 (2003).
15. K. S. Yan *et al.*, *Nature* **426**, 468 (2003).
16. A. Boland, F. Tritschler, S. Heimstädt, E. Izaurralde, O. Weichenrieder, *EMBO Rep.* **11**, 522 (2010).
17. A. Boland, E. Huntzinger, S. Schmidt, E. Izaurralde, O. Weichenrieder, *Proc. Natl. Acad. Sci. U.S.A.* **108**, 10466 (2011).
18. F. Frank, N. Sonenberg, B. Nagar, *Nature* **465**, 818 (2010).
19. Y. L. Chiu, T. M. Rana, *RNA* **9**, 1034 (2003).
20. G. F. Deleavey *et al.*, *Nucleic Acids Res.* **38**, 4547 (2010).
21. D. P. Bartel, *Cell* **116**, 281 (2004).
22. B. P. Lewis, C. B. Burge, D. P. Bartel, *Cell* **120**, 15 (2005).
23. D. P. Bartel, *Cell* **136**, 215 (2009).
24. S. L. Lian *et al.*, *RNA* **15**, 804 (2009).
25. A. Eulalio, S. Helms, C. Fritzsch, M. Fauser, E. Izaurralde, *RNA* **15**, 1067 (2009).
26. M. El-Shami *et al.*, *Genes Dev.* **21**, 2539 (2007).
27. N. Bies-Etheve *et al.*, *EMBO Rep.* **10**, 649 (2009).
28. D. Baillat, R. Shiekhattar, *Mol. Cell. Biol.* **29**, 4144 (2009).
29. S. Till *et al.*, *Nat. Struct. Mol. Biol.* **14**, 897 (2007).

Acknowledgments: We thank the laboratories of D. Stout, E. O. Saphire, and I. Wilson for sharing synchrotron time and for helpful discussions. Crystallization screens were carried out at the Joint Center for Structural Genomics, supported by the National Institute of General Medical Sciences (NIGMS) Protein Structure Initiative (U54 GM074898). Diffraction data were collected on beamlines 24-ID-E at the Advanced Photon Source and 11-1 at the Stanford Synchrotron Radiation Lightsource. This work was supported by NIGMS grant R01 GM086701 to I.J.M. I.J.M. is a Pew Scholar in the Biomedical Sciences. Coordinates of Ago2 and Ago2 bound to tryptophan have been deposited in the Protein Data Bank (4EI1 and 4EI3).

Supplementary Materials

www.sciencemag.org/cgi/content/full/science.1221551/DC1
Materials and Methods
Figs. S1 to S15
Tables S1 and S2
References (*30*–*38*)

6 March 2012; accepted 17 April 2012
Published online 26 April 2012;
10.1126/science.1221551

Metabolite Profiling Identifies a Key Role for Glycine in Rapid Cancer Cell Proliferation

Mohit Jain,[1,2,3,4]* Roland Nilsson,[1,2,3,5]* Sonia Sharma,[6] Nikhil Madhusudhan,[1,2,3] Toshimori Kitami,[1,2,3] Amanda L. Souza,[1] Ran Kafri,[2] Marc W. Kirschner,[2] Clary B. Clish,[1] Vamsi K. Mootha[1,2,3]†

Metabolic reprogramming has been proposed to be a hallmark of cancer, yet a systematic characterization of the metabolic pathways active in transformed cells is currently lacking. Using mass spectrometry, we measured the consumption and release (CORE) profiles of 219 metabolites from media across the NCI-60 cancer cell lines, and integrated these data with a preexisting atlas of gene expression. This analysis identified glycine consumption and expression of the mitochondrial glycine biosynthetic pathway as strongly correlated with rates of proliferation across cancer cells. Antagonizing glycine uptake and its mitochondrial biosynthesis preferentially impaired rapidly proliferating cells. Moreover, higher expression of this pathway was associated with greater mortality in breast cancer patients. Increased reliance on glycine may represent a metabolic vulnerability for selectively targeting rapid cancer cell proliferation.

Malignant transformation results from mutations that alter cellular physiology to confer a proliferative advantage (*1*, *2*). Despite the genetic heterogeneity and complexity of cancer (*3*), transformed cells exhibit a limited number of proposed common hallmarks, including metabolic reprogramming, which manifests as altered nutrient uptake and use (*2*, *4*). Although metabolic reprogramming is thought to be essential for rapid cancer cell proliferation, a systematic characterization of the metabolic pathways active in transformed cells is lacking, and the contribution of these pathways in promoting rapid cancer cell proliferation remains unclear (*4*). Existing studies of cancer metabolism have examined relatively few cell lines, and have largely focused on the measurement of intracellular metabolite pools (*5*)—from which it is difficult to infer metabolic pathway activity—or have relied on isotope tracing to estimate metabolic flux through a limited number of reactions (*6*).

To systematically characterize cancer cell metabolism, we used liquid chromatography–tandem mass spectrometry (LC-MS/MS) to create cellular consumption and release (CORE) profiles of 219 metabolites (table S1) spanning the major pathways of intermediary metabolism, in the NCI-60 panel, a collection of 60 well-characterized primary human cancer cell lines established from nine common tumor types (*7*). CORE profiling builds on metabolic footprinting or exometabolomics (*8*, *9*), and provides a systematic and quantitative assessment of cellular metabolic activity by relating metabolite concentrations in spent medium from cultured cells to metabolite concentrations in baseline medium, resulting in a time-averaged CORE profile for each metabolite on a per-cell basis over a period of exponential growth (Fig. 1). Using CORE profiling, we identified 140 metabolites that were either present in fresh medium or released by at least one cancer cell line, of which 111 metabolites demonstrated appreciable variation across the 60 cell lines, with excellent reproducibility between biological replicates (Fig. 2). About one-third of the 111 metabolites were consumed by all cell lines, whereas most of the remaining two-thirds of metabolites were consistently released into the medium; only a handful of metabolites exhibited consumption in certain cell lines and release by others (Fig. 2). A larger, fully annotated version of Fig. 2 is provided in fig. S1.

This CORE atlas of cancer metabolism (Fig. 2 and fig. S1) can be used to explore metabolic phenotypes of cancer cells and to discover relationships between metabolites. For example, ornithine was released from leukemia cells, and adenosine and inosine were released from melanoma cells (fig. S2), reflecting metabolic activities that may be unique to these cancers. Unsupervised cluster analysis of metabolite

[1]Broad Institute, Cambridge, MA 02142, USA. [2]Department of Systems Biology, Harvard Medical School, Boston, MA 02115, USA. [3]Center for Human Genetic Research and Department of Molecular Biology, Massachusetts General Hospital, Boston, MA 02114, USA. [4]Division of Cardiovascular Medicine, Department of Medicine, Brigham and Women's Hospital, Boston, MA 02115, USA. [5]Unit of Computational Medicine, Department of Medicine, Karolinska Institutet, 17176 Stockholm, Sweden. [6]La Jolla Institute for Allergy & Immunology, La Jolla, CA 92037, USA.

*These authors contributed equally to this work.
†To whom correspondence should be addressed. E-mail: vamsi@hms.harvard.edu

CORE data identified leukemia cells as a distinct group but did not more generally distinguish between tumor cell lines according to tissue of origin (fig. S3). Functionally related metabolites demonstrated similar patterns of consumption and release across the 60 cell lines. For example, major nutrients including glucose, essential amino acids, and choline formed a single cluster, as did metabolites representing glycolysis, the citric acid cycle, nucleotides, and polyamines (Fig. 2 and fig. S1). Consumption of major nutrients also correlated with release of their by-products; for example, glucose consumption correlated to lactate release (Fig. 1B), consistent with the well-documented Warburg effect in transformed cells (*4*). A similar pattern of nutrient consumption and by-product release was also observed with other nutrients. Glutamine consumption, quantitatively the greatest among amino acids, was closely mirrored by glutamate release (Fig. 1B). An analysis of all monitored metabolites revealed that total measured carbon consumption was also closely correlated with total measured carbon release (Fig. 1B), which suggests that transformed cells share a common metabolic phenotype: incomplete catabolism of major nutrients followed by release of by-products.

We next sought to determine whether any metabolite CORE profiles were associated with cancer cell proliferation. Previously reported doubling times across the 60 cancer cell lines ranged from 17.0 to 79.5 hours and were highly reproducible (*10*) (fig. S4). From the 111 metabolite CORE profiles, two metabolites—phosphocholine and glycine—were significantly correlated (Bonferroni-corrected $P < 0.01$) with proliferation rate across the 60 cell lines (Fig. 3A). Phosphocholine, which was released from all cells, correlated with consumption of the essential nutrient choline (fig. S5) and has been reported to accumulate in transformed cells as a substrate for phospholipid biosynthesis (*11*). In contrast, the relation between glycine consumption and proliferation rate was unanticipated, because glycine is a non-essential amino acid that can be endogenously synthesized. Glycine exhibited an unusual CORE profile, being consumed by rapidly proliferating cells and released by slowly proliferating cells (Fig. 3B), which suggests that glycine demand may exceed endogenous synthesis capacity in rapidly proliferating cancer cells, whereas in slowly proliferating cells, glycine synthesis may exceed demand. Increasing glycine consumption with faster proliferation rate was observed across all 60 cell lines (Fig. 3B) and was even more pronounced within specific tumor types, including ovarian, colon, and melanoma cells (Fig. 3B and fig. S6), but was not evident in nonadherent leukemia cells (fig. S6).

To determine whether glycine consumption is specific to transformed cells or a general feature of rapid proliferation, we measured glycine consumption in cultured primary human mammary epithelial cells (HMECs), human bronchial epithelial (HBE) cells, human umbilical vein endothelial cells (HUVECs), and human activated $CD4^+$ T lymphocytes. These nontransformed cells had doubling times between 8 and 18 hours, comparable to the most rapidly dividing cancer cells, yet each of these cell types released rather than consumed glycine (HMECs, 3.5 ± 0.8 fmol $cell^{-1}$ $hour^{-1}$; HBE cells, 17.5 ± 3.2 fmol $cell^{-1}$ $hour^{-1}$; HUVECs, 8.4 ± 1.4 fmol $cell^{-1}$ $hour^{-1}$; lymphocytes, 1.9 ± 0.3 fmol $cell^{-1}$ $hour^{-1}$). Thus, glycine consumption appears to be a feature specific to rapidly proliferating transformed cells.

To complement the metabolite CORE analysis, we next examined the gene expression of 1425 metabolic enzymes (*12*) in a previously generated microarray data set across these 60 cell lines (*13*). This independent analysis revealed that glycine biosynthesis enzymes are more highly expressed in rapidly proliferating cancer cell lines (Fig. 3C). Intracellular glycine synthesis is compartmentalized between the cytosol and mitochondria (*14*), providing two separate enzymatic pathways (Fig. 3D). The mitochondrial glycine synthesis pathway consists of the glycine-synthesizing enzyme serine hydroxymethyltransferase 2 (SHMT2), a target of the oncogene c-Myc (*15*), as well as MTHFD2 and MTHFD1L, which regenerate the cofactor tetrahydrofolate (THF) for the SHMT2 reaction (Fig. 3D). The mitochondrial pathway exhibited significant correlation with proliferation, whereas the corresponding cytosolic enzymes did not (Fig. 3C), which suggests a key role for mitochondria in supporting rapid cancer cell proliferation. To assess the relative contributions of glycine consumption and endogenous synthesis to intracellular glycine pools, we used tracer analysis with (^{13}C)glycine in rapidly dividing LOX IMVI cells. Assuming a simple steady-state model (*13*), we estimate from labeling of intracellular glycine and serine pools (Fig. 3E) that about one-third of intracellular glycine originates from extracellular consumption, whereas the remainder is synthesized endogenously. Thus, both metabolite CORE profiling and gene expression analysis independently identify glycine metabolism as closely related to rapid proliferation in cancer cells.

To directly evaluate the contribution of glycine metabolism to rapid cancer cell proliferation, we used a combination of genetic silencing and nutrient deprivation. We stably silenced expression of the glycine-synthesizing enzyme SHMT2 in slowly proliferating A498 cells and in rapidly proliferating LOX IMVI cells (Fig. 3B) with four distinct short hairpin RNA (shRNA) sequences (fig. S7A). Chinese hamster ovary cell strains mutant in SHMT2 were previously shown to be auxotrophic for glycine (*16*). Silencing of SHMT2 in the absence of extracellular glycine halted the proliferation of LOX IMVI cells (Fig. 3F) and was rescued by the addition of glycine to the medium; this indicates that glycine itself, rather than one-carbon units derived from the SHMT2 reaction (Fig. 3D), is critical to proliferation in these cells (Fig. 3F). Supplementation of medium with sarcosine, a glycine-related metabolite (*17*), or formate, a source of cellular one-carbon units (*18*), failed to rescue LOX IMVI cells (fig. S7B). In contrast, slowly proliferating A498 cells (Fig. 3F) were not impaired by SHMT2 depletion and extracellular glycine deprivation, indicating that other means of glycine synthe-

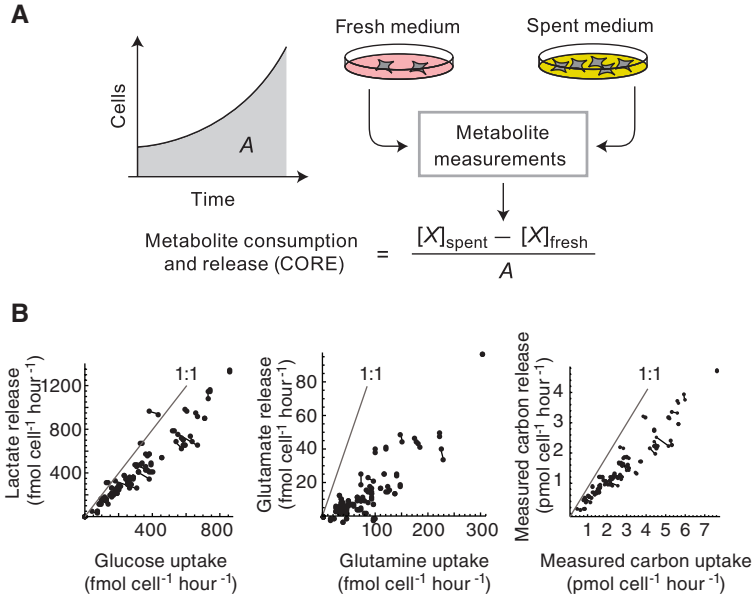

Fig. 1. CORE profiling. (**A**) For determining metabolite CORE (consumption and release) profiles, medium samples taken before (fresh) and after (spent) 4 to 5 days of cell culture are subjected to metabolite profiling by LC-MS/MS. For each metabolite *X*, the CORE value is calculated as the difference in molar abundance normalized to the area *A* under the growth curve. (**B**) Glucose consumption versus lactate release, glutamine consumption versus glutamate release, and total measured carbon consumption versus total measured carbon release across the 60 cell lines. Gray lines indicate the 1:1 molar ratio (carbon consumed/carbon released) for each metabolite pair; joined data points represent biological replicates.

sis can satisfy the requirements in these cells. Withdrawal of extracellular glycine alone also reduced the proliferation of LOX IMVI cells but not A498 cells (fig. S8), although this effect was more subtle. Collectively, our data suggest that mitochondrial production of glycine is critical specifically in rapidly proliferating cancer cells. To determine whether this reliance on glycine for rapid proliferation extends to other cancer cells, we tested silencing of SHMT2 (fig. S7C) and extracellular glycine deprivation in 10 additional primary cancer cell lines from the NCI-60 panel (Fig. 3G). Rapidly proliferating cancer cells exhibited slower proliferation with antagonism of glycine metabolism and were rescued with addition of extracellular glycine, whereas slowly proliferating cells were less sensitive to these perturbations (Fig. 3G), even when assessed at later time points to allow for a comparable number of cellular divisions relative to rapidly proliferating cells (fig. S9).

We next sought to explore the potential mechanisms by which glycine metabolism contributes to rapid cancer cell proliferation. Metabolic tracing with (^{13}C)glycine revealed that consumed glycine was incorporated into purine nucleotides in rapidly proliferating LOX IMVI cells, but less so in slowly proliferating A498 cells (Fig. 4, A and B), which suggests that consumed glycine in part supports de novo purine synthesis in these cells. We also noted the incorporation of labeled glycine into cellular glutathione (fig. S10A). Analysis of previously performed large-scale chemosensitivity profiling across the 60 cancer cell lines (*7*) revealed that sensitivity to an inhibitor of glutathione synthesis, buthionine sulfoximine (*19*), was unrelated to proliferation rate (fig. S10B), whereas sensitivity to inhibitors of de novo purine biosynthesis—mycophenolate, tiazofurin, and alanosine (*20*)—was highly correlated with proliferation rate across the cell lines (fig. S10C). The use of glycine for de novo purine biosynthesis can occur by two mechanisms: direct incorporation into the purine backbone, or further oxidation by the glycine cleavage system (GCS) to yield one-carbon units for nucleotide synthesis and cellular methylation reactions (Fig. 4A). Because only carbon 2 of glycine is converted into one-carbon units by the GCS (Fig. 4A), we cultured LOX cells in 1-(^{13}C)glycine or 2-(^{13}C)glycine to differentiate between these two mechanisms (*21*). Consumed 2-(^{13}C)glycine did not give rise to doubly labeled purines (Fig. 4B), which indicates that the incorporation of consumed glycine into purine nucleotides does not involve oxidation by the GCS.

To better characterize the impact of glycine deprivation on cell cycle progression, we performed cell cycle analysis in HeLa cancer cells expressing a geminin–green fluorescent protein reporter and stained with DAPI (4′,6-diamidino-2-phenylindole). Silencing of SHMT2 (fig. S11A) and deprivation of extracellular glycine slowed proliferation in HeLa cells (fig. S11B), similar to other fast-proliferating cancer cells (Fig. 3G), and resulted in prolongation of the G_1 phase of the cell cycle (Fig. 4C and fig. S11C), whereas protein synthesis remained relatively intact (fig. S11D), consistent with a defect in nucleotide biosynthesis (*20*). Collectively, these results suggest that consumed glycine is used in part for de novo purine nucleotide biosynthesis in rapidly proliferating cells, and that antagonism of glycine metabolism results in prolongation of the G_1 phase, thus slowing proliferation.

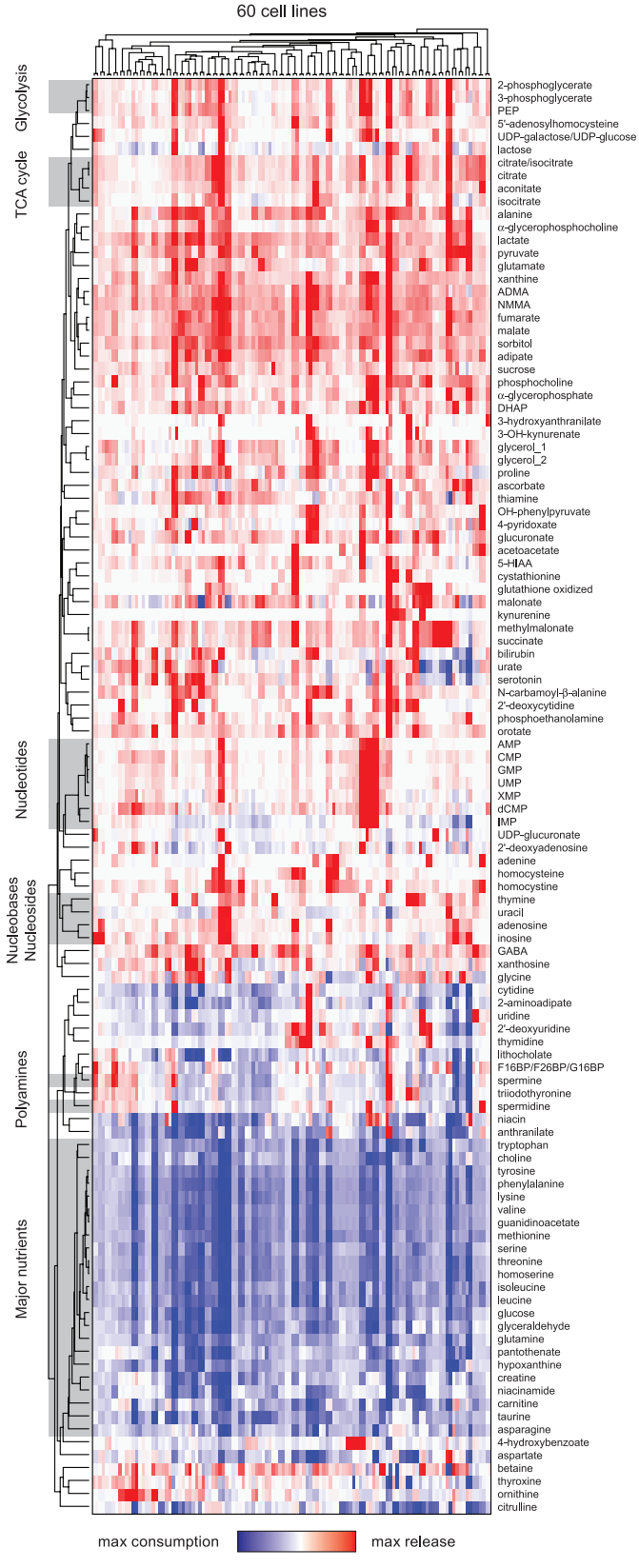

Fig. 2. CORE profiling across the NCI-60 cell lines. Hierarchical clustering of CORE profiles for 111 metabolites across 60 cancer cell lines in duplicate cultures, are shown; blue color indicates consumption, white indicates no change, and red color indicates release. Gray highlights indicate functionally related metabolites. In three rows, metabolites that cannot be distinguished are separated by slashes. Glycerol_1 and glycerol_2 represent independent LC-MS/MS measures.

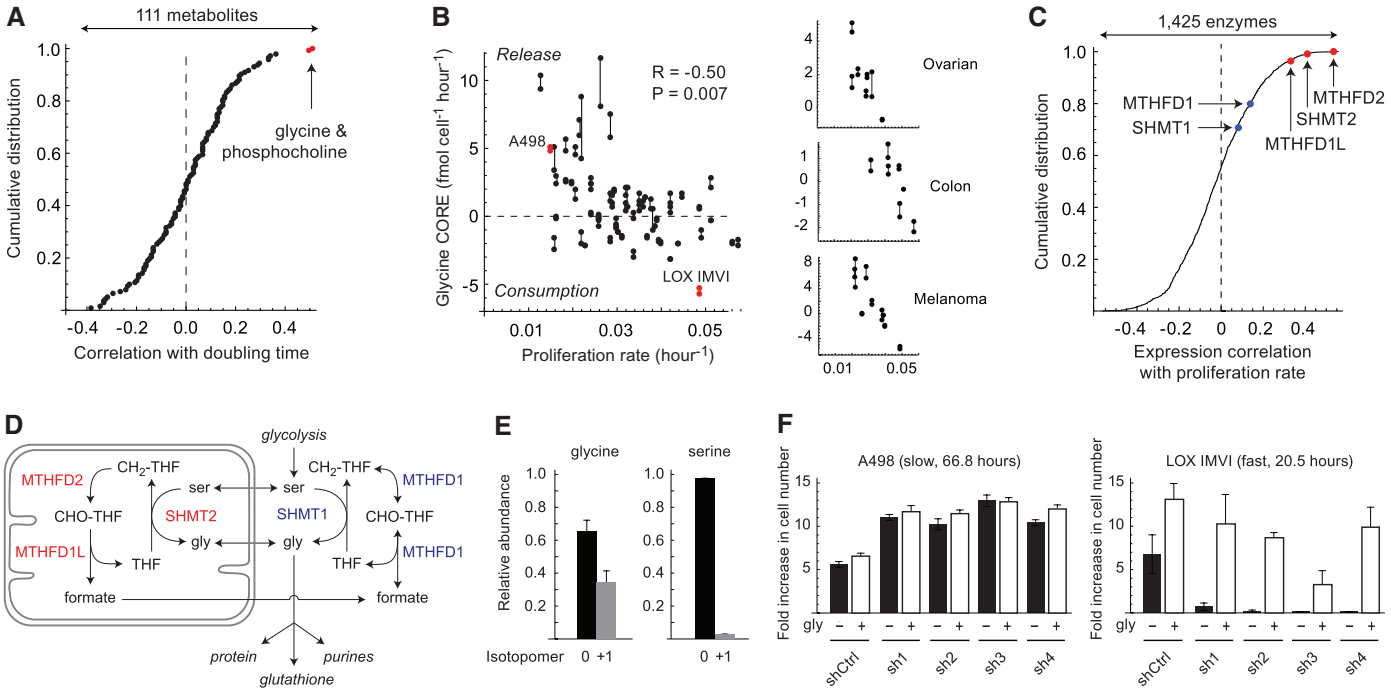

Fig. 3. Glycine consumption and synthesis are correlated with rapid cancer cell proliferation. (**A**) Distribution of Spearman correlations between 111 metabolite CORE profiles and proliferation rate across 60 cancer cell lines. Only metabolites highlighted in red are significant at $P < 0.05$, Bonferroni-corrected. (**B**) Glycine CORE versus proliferation rate across 60 cancer cell lines (left) and selected solid tumor types (right). Cell lines selected for follow-up experiments are highlighted in red. Joined data points represent replicate cultures. *P* values are Bonferroni-corrected for 111 tested metabolites. (**C**) Distribution of Spearman correlations between gene expression of 1425 metabolic enzymes and proliferation rates across 60 cancer cell lines. Highlighted are mitochondrial (red) and cytosolic (blue) glycine metabolism enzymes. (**D**) Schematic of cytosolic and mitochondrial glycine metabolism. (**E**) Abundance of unlabeled (0) and labeled (+1) intracellular glycine and serine in LOX IMVI cells grown on 100% extracellular (^{13}C)glycine. (**F**) Growth of A498 and LOX IMVI cells expressing shRNAs targeting SHMT2 (sh1-4) or control shRNA (shCtrl), cultured in the absence (solid bars) or presence (open bars) of glycine (gly). (**G**) Growth of 10 cancer cell lines expressing shRNA targeting SHMT2 (sh4) after 3 days, cultured in the absence (–gly, solid bars) or presence (+gly, open bars) of glycine. Cell number is presented as a ratio relative to +gly cells. Error bars in (E), (F), and (G) denote SD.

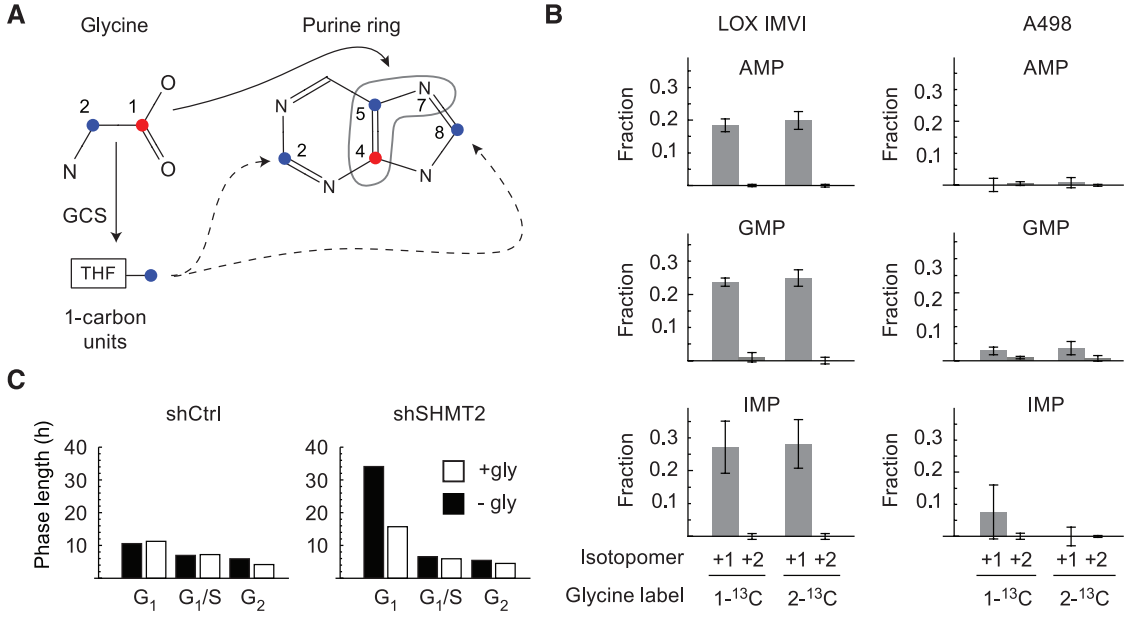

Fig. 4. Glycine metabolism supports de novo purine nucleotide biosynthesis. (**A**) Schematic of carbon incorporation into the purine ring from 1-(^{13}C)glycine or 2-(^{13}C)glycine. THF, tetrahydrofolate; GCS, glycine cleavage system. (**B**) Purine nucleotide +1 and +2 isotopomers in LOX IMVI or A498 cells grown on 100% 1-(^{13}C)glycine or 2-(^{13}C)glycine, as a fraction of the total intracellular metabolite pool. (**C**) Cell cycle analysis in HeLa cells expressing shRNA targeting SHMT2 (shSHMT2) or control shRNA (shCtrl), grown in the absence (–gly, solid bars) or presence (+gly, open bars) of glycine. Cell cycle phase length was calculated from the percentage of cells present in each cell cycle phase by geminin expression and DAPI staining (fig. S11C).

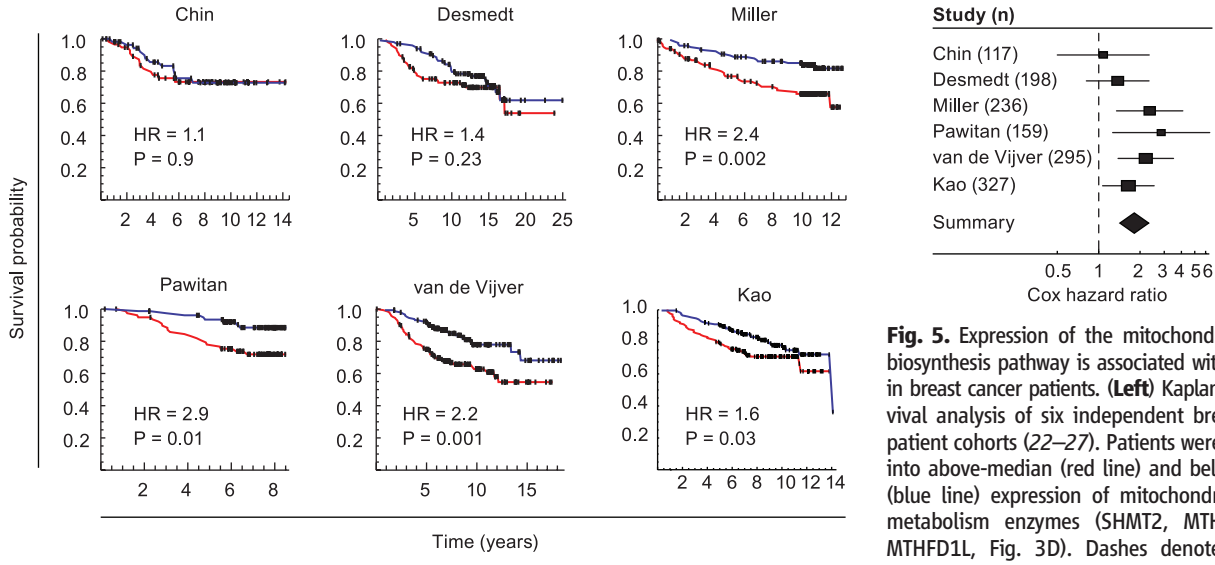

Fig. 5. Expression of the mitochondrial glycine biosynthesis pathway is associated with mortality in breast cancer patients. (**Left**) Kaplan-Meier survival analysis of six independent breast cancer patient cohorts (*22*–*27*). Patients were separated into above-median (red line) and below-median (blue line) expression of mitochondrial glycine metabolism enzymes (SHMT2, MTHFD2, and MTHFD1L, Fig. 3D). Dashes denote censored events. (**Right**) Meta-analysis of Cox hazard ratios for the six studies. Solid lines denote 95% confidence intervals; boxes denote the relative influence of each study over the results (inverse squared SE); diamond marks the overall 95% confidence interval.

To explore the potential relevance of glycine metabolism to cancer, we examined the expression of the mitochondrial glycine synthesis enzymes SHMT2, MTHFD2, and MTHFD1L (Fig. 3D) in previously generated microarray data sets across six independent large cohorts totaling more than 1300 patients with early-stage breast cancer followed for survival (*22*–*27*). We defined two groups of individuals: those with above-median gene expression of the mitochondrial glycine biosynthesis pathway, and those with below-median gene expression. Above-median expression of the mitochondrial glycine biosynthesis pathway was associated with greater mortality (Fig. 5), and a formal meta-analysis of all six data sets indicated an overall hazard ratio of 1.82 (95% confidence interval, 1.43 to 2.31; Fig. 5), comparable to those of other established factors, such as lymph node status and tumor grade, that contribute to poor cancer prognosis (*25*). The mitochondrial glycine synthesis enzyme SHMT2 alone was also significantly associated with mortality, whereas its cytosolic paralog SHMT1 was not (fig. S12). These data highlight the potential importance of mitochondrial glycine metabolism in human breast cancer.

Our atlas of cancer cell metabolism generated by CORE profiling may be broadly useful for investigating cellular metabolism and for identifying metabolite biomarkers of cancer and drug responsiveness. In our study, we used this atlas to probe the relation between metabolism and proliferation, thereby discovering an unexpected increased reliance on glycine metabolism in rapidly proliferating cancer cells—a phenotype that was not observed in rapidly proliferating nontransformed cells. Although we found that glycine is used for de novo purine nucleotide biosynthesis in rapidly proliferating LOX IMVI cells, alternative mechanisms—including the use of one-carbon groups derived from glycine for cellular methylation reactions (*17*)—may be important in other cancer cell types. Glycine and related metabolites (including sarcosine, serine, and threonine), or their associated metabolic pathways, have been identified as central to cancer metastasis (*5*), cellular transformation (*17*, *28*, *29*), and murine embryonic stem cell proliferation (*30*). Glycine metabolism may therefore represent a metabolic vulnerability in rapidly proliferating cancer cells that could in principle be targeted for therapeutic benefit.

References and Notes

1. P. C. Nowell, *Science* **194**, 23 (1976).
2. D. Hanahan, R. A. Weinberg, *Cell* **144**, 646 (2011).
3. M. R. Stratton, P. J. Campbell, P. A. Futreal, *Nature* **458**, 719 (2009).
4. P. P. Hsu, D. M. Sabatini, *Cell* **134**, 703 (2008).
5. A. Sreekumar *et al.*, *Nature* **457**, 910 (2009).
6. R. J. DeBerardinis *et al.*, *Proc. Natl. Acad. Sci. U.S.A.* **104**, 19345 (2007).
7. R. H. Shoemaker, *Nat. Rev. Cancer* **6**, 813 (2006).
8. J. Allen *et al.*, *Nat. Biotechnol.* **21**, 692 (2003).
9. O. Shaham *et al.*, *Proc. Natl. Acad. Sci. U.S.A.* **107**, 1571 (2010).
10. P. M. O'Connor *et al.*, *Cancer Res.* **57**, 4285 (1997).
11. R. Katz-Brull, H. Degani, *Anticancer Res.* **16**, 1375 (1996).
12. N. C. Duarte *et al.*, *Proc. Natl. Acad. Sci. U.S.A.* **104**, 1777 (2007).
13. See supplementary materials on *Science* Online.
14. A. S. Tibbetts, D. R. Appling, *Annu. Rev. Nutr.* **30**, 57 (2010).
15. M. A. Nikiforov *et al.*, *Mol. Cell. Biol.* **22**, 5793 (2002).
16. F. Kao, L. Chasin, T. T. Puck, *Proc. Natl. Acad. Sci. U.S.A.* **64**, 1284 (1969).
17. W. C. Zhang *et al.*, *Cell* **148**, 259 (2012).
18. H. Patel, E. D. Pietro, R. E. MacKenzie, *J. Biol. Chem.* **278**, 19436 (2003).
19. O. W. Griffith, A. Meister, *J. Biol. Chem.* **254**, 7558 (1979).
20. S. P. Linke, K. C. Clarkin, A. Di Leonardo, A. Tsou, G. M. Wahl, *Genes Dev.* **10**, 934 (1996).
21. T. F. Fu, J. P. Rife, V. Schirch, *Arch. Biochem. Biophys.* **393**, 42 (2001).
22. K. Chin *et al.*, *Cancer Cell* **10**, 529 (2006).
23. C. Desmedt *et al.*; TRANSBIG Consortium, *Clin. Cancer Res.* **13**, 3207 (2007).
24. Y. Pawitan *et al.*, *Breast Cancer Res.* **7**, R953 (2005).
25. M. J. van de Vijver *et al.*, *N. Engl. J. Med.* **347**, 1999 (2002).
26. K. J. Kao, K. M. Chang, H. C. Hsu, A. T. Huang, *BMC Cancer* **11**, 143 (2011).
27. L. D. Miller *et al.*, *Proc. Natl. Acad. Sci. U.S.A.* **102**, 13550 (2005).
28. R. Possemato *et al.*, *Nature* **476**, 346 (2011).
29. J. W. Locasale *et al.*, *Nat. Genet.* **43**, 869 (2011).
30. J. Wang *et al.*, *Science* **325**, 435 (2009).

Acknowledgments: We thank T. R. Golub, O. Shaham, S. B. Vafai, and L. Strittmatter for scientific discussions and feedback; X. Cao for assistance with glucose and lactate measurements; the Broad Institute RNAi Platform for shRNA reagents; D. Gomez-Cabrero for assistance with multidimensional scaling; A. Ploner and P. Dickman for assistance with survival analysis; W. C. Kopp, S. L. Holbeck, K. Gill, and P. Sellers of the Developmental Therapeutics Program, National Cancer Institute, for reagents and assistance with cell culture; and T. Hasaka of the Broad Institute for assistance with imaging studies. Supported by NIH grant K08HL107451 (M.J.), a postdoctoral scholarship from the Knut & Alice Wallenberg Foundation and Stockholm County (SLL) grant 01626-2009 (R.N.), a Special Fellow award from the Leukemia & Lymphoma Society (S.S.), and NIH grant R01DK081457 and a gift from the Nestle Research Center (V.K.M.). The full metabolite CORE profiling data set is available in the supplementary materials as well as through the NCI Molecular Targets data repository (http://dtp.nci.nih.gov/mtargets/download.html). M.J. and R.N. conceived and performed all experiments, collected and analyzed experimental data, and prepared the manuscript. S.S. assisted with cell culture, RNAi, and T lymphocyte experiments. N.M. and T.K. assisted with cell culture and imaging-based experiments. A.L.S. and C.B.C. performed LC-MS/MS profiling experiments and provided experimental feedback. R.K. and M.W.K. performed cell cycle studies. V.K.M. conceived all experiments, reviewed all experimental data, and prepared the manuscript. All authors have discussed the results and reviewed the manuscript. All authors declare no competing financial interests.

Supplementary Materials

www.sciencemag.org/cgi/content/full/336/6084/1040/DC1
Materials and Methods
Figs. S1 to S12
Table S1
References (*31*–*43*)
Database S1

8 July 2011; accepted 23 March 2012
10.1126/science.1218595